This article has been accepted for publication in a future issue of this journal, but has not been fully edited. Content may change prior to final publication. Citation information: DOI 10.1109/JRFID.2017.2765619, IEEE Journal of Radio Frequency Identification

The Interrogation Footprint of RFID-UAV: Electromagnetic Modeling and Experimentations

G. Casati, M. Longhi, D. Latini, F. Carbone, S. Amendola, F. Del Frate, G. Schiavon and G. Marrocco

***Abstract*—The combined use of Unmanned Aerial Vehicles and Radiofrequency Identification devices is an emerging topic of the environmental monitoring, which combines the versatility of multi-copter airframes with the potentiality of low-cost wireless sensors. This paper introduces some performance metrics suitable to quantify the capability of an *RFIDrone* to scan a surface equipped with radio-sensors. By using simple propagation models, an optimal drone-surface distance is mathematically derived at the purpose to maximize the electromagnetic footprint for the specific choice of system parameters, such as the sensor type and position, the reader sensitivity, the ground reflectivity, the radiated power and the flight velocity. Theoretical achievements and some preliminary experimentations indicate that omnidirectional antennas are preferred for the drone so that 9-12m footprints could be achieved with state-of-the-art readers and battery-less or battery-assisted RFID sensors, provided that the UAV flights at 3-5 m from the surface to be monitored. In this condition, the hit-rate of arrays of tags is better than 90% for a flying speed less than 1.8 Km/h. The read performance is instead sensibly degraded by the presence of multi path in case of sensors spaced out the surface.**

***Index Terms*—Radiofrequency Identification, UAV, Drone, Structural Health Monitoring, Internet of Things, Smart Buildings.**

I. Introduction[1]

Radiofrequency Identification (RFID) technology is currently orienting from logistic-only applications toward more higher-value sensing systems, hence becoming one of the enabling technologies of the Internet of Things [1]. At a same time, Unmanned Aerial Vehicles (UAV) are experiencing a huge growth in both amateur and professional contexts involving micro-drones with very limited autonomy up to small multi-rotor air frames with long-range scope [2], [3]. RFID and UAV technologies are now mature to be merged together thus enabling a set of completely new opportunities. A few researchers and companies have already envisaged this potentiality and some very preliminary experimentations may be found over conventional scientific channels. It is conceived that an UAV could be equipped with an RFID scanner in the UHF band [4] and this moving agent could locate and collect identification and sensing information from RFID tags displaced in harsh environments [5] like bridges [6], viaducts [7], outdoor environments [8] and outdoor warehouses [9], [10]. Accordingly, the preliminary envisaged applications are Structural Health Monitoring [11], Precise Agriculture [12], Automated Inventory in large areas [13]–[15], Asset Management [16] and Animal Surveillance [17].

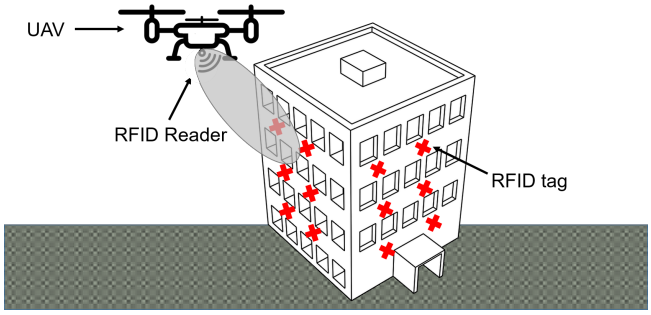

Figure 1. RFIDrone hosting an RFID reader and interacting with fixed sensors displaced over an infrastructure.

The RFID-UAV research field, hereafter referred to as *RFIDrone,* is however in its infancy. An RFIDrone infrastructure involves specific features, with respect to standard ground-level inventory and sensing, such as: *i*) the very limited power budget, allowing for only short reading sessions, *ii*) tags placed at a very close distance from a large surface, or directly attached over it, *iii*) a moving agent and *iv*) the need to quickly approach the tags from a remote distance. Unlike onboard cameras, that can be considered as remote-sensing devices, RFID readers are instead short-range scanning systems that require the UAV to fly at a few meters distance from the sensors. The challenge is definitely locating small objects (the sensor tags) within a large and complex environment. As discussed in [3], the GPS-assisted guide is useful to approach the approximate location of the tag, but, due to the limited resolution of the GPS, the drone (UAV) is currently unable to autonomously get close enough to the sensors to establish a reliable RFID communication link. Accordingly, the final approach to the tags is based on a manual/assisted short-range RFID radar scanning the surface and hence the onboard RFID reader and its power has to be used in an optimal way. An open question, in particular, concerns the best UAV-surface distance capable to maximize the number of identified tags and, more in general, to reduce the scanning time.

[1]Manuscript submitted on January 19th 2017. Authors are with the Department of Civil and Informatics Engineering, University of Roma Tor Vergata, Via del Politecnico, 1 00133, Roma (IT). Reference mail: gaetano.marrocco@uniroma2.it.

This article has been accepted for publication in a future issue of this journal, but has not been fully edited. Content may change prior to final publication. Citation information: DOI 10.1109/JRFID.2017.2765619, IEEE Journal of Radio Frequency Identification

So far, the impact of an RFIDrone system parameters (the deployed sensors, the onboard reading device) on the scan reliability, has been not yet clarified. Therefore, following the preliminary discussions in [18], this contribution aims at introducing performance metrics and to derive their upper bounds for the interrogation of battery-less and battery-assisted tags from a flying reader. The study considers some possible scenarios where tags are directly attached on a surface (as in case of buildings) or are displaced at a certain distance from it (agriculture monitoring). The concept of RFIDrone's footprint is introduced together with conditions to maximize it.

The paper is organized as follows. In Section II, the RFIDrone system architecture is described and some indicators are proposed to quantify the size of the read region and the read reliability when sensors are distributed in the environment. Section III introduces the footprint of the RFIDrone and its optimal values with respect to all the electrical and geometrical parameters of the scanning system. A preliminary experimental corroboration is given in Section IV by the help of a static configuration where all the geometrical parameters were well controlled. Finally, Section V resumes a realistic test case with a flying RFIDrone interrogating both battery-less and battery-assisted tags.

II. The RFIDrone System

The RFIDrone system consists of a suitable UAV hosting an autonomous RFID reader to act as mobile scanner of the environment (Fig. 1). The drone can be manually or automatically driven by remote to approach tags displaced on a surface and retrieve the sensed data. The drone could also profit from beacon tags to improve self-localization [19], especially around obstacles. Sampled data may be stored onboard for a later-time recovery when the drone comes back, or real-time transmitted to a fixed base-station placed in radio visibility with the drone itself.

A. Application Scenarios

Two principal macro-scenarios have been identified by considering the role of the position of tags w.r.t. the environment:

1) *Monitoring of surfaces (tags-on-surfaces)*: the sensor-equipped tags are distributed on the surface of large objects, such as concrete walls or metal structures, for sensing purposes (i.e. structural health monitoring). Tags are embedded in the structures and the RFIDrone is used to fly parallel to the surfaces in order to download data from the tags.
2) *Monitoring of objects close to surfaces (spaced-out tags)*: sensor-equipped tags are positioned at a given distance from a large object, for example the soil. This may occur in applications such as precision farming, when tags are provided with a probe inserted into the soil or hanged on trees.

In the second case, the effect of multi-path due to the reflection from the ground of the interrogating electromagnetic waves coming from the drone, is supposed to introduce a performance degradation, as shown later on.

B. Performance indicators

The performance of an RFID interrogation system is determined by the reading region of the reader, e.g. the volume of space around the reader's antenna wherein tags receive enough energy to activate and establish a robust communication link with the reader [20]. Such read volume can be approximated by an ellipsoid whose axis are related to the nearby environment, the power emitted by the reader and the gain of its antenna, the reader and the tag sensitivity, the radiation patterns and the mutual orientation of the antennas. Ultimately, an assessed overall performance indicator of an RFID link is the maximum read distance of the specific tag.

In the RFIDrone scenario, as tags are expected to be displaced on surfaces, a possible performance indicator is the reader *Footprint* (FP), i.e. the surface of intersection between the read volume and the plane passing through the tags. The footprint is related to the ability of an RFIDrone framework to detect sensors over the surface of interest in the shortest possible time in order to comply with its limited power autonomy. The larger the footprint, the easier will be the discovery of a tag and the shorter the time required to complete the environment inventory and monitoring. In particular, we consider the footprint as the performance parameter of the RFIDrone interrogation and we expect that such a size will have a non-monotonic dependence with the UAV-ground distance. Accordingly, an optimum flight altitude could exist for which the footprint size is maximized.

While the FP gives an indication about the time required by the UAV to scan a given surface, the number of instantaneously read tags is quantified by the Hit-Rate (HR) [21] indicator which is conventionally used in logistics. This parameter gives the percentage of the responding tags normalized by the total number of tags inside the footprint of the reader and is strictly correlated to the speed of the RFIDrone:

$$HR\,(v) = \frac{n(v)}{N_{FP}} \tag{1}$$

where n is the average number of readings at speed v and N_{FP} the average number of total tags within the footprint calculated from the density of tags ρ_T ($[1/m^2]$):

$$N_{FP} = \rho_T \cdot FP. \tag{2}$$

Hence, the maximum number of tags illuminated within the footprint is directly proportional to the optimal footprint. The HR permits to derive the most appropriate speed of the UAV during the scan as it will be shown in the experimental Sections.

III. Footprint Representation

RFID communication comprises a forward-link (from the reader to the tag) and a backward-link (from the tag to the reader) [22]. By preliminary assuming free-space conditions, the RFID links are governed by the Friis formula and by the Radar Equation, respectively. Denoting with P_R and P_C the

This article has been accepted for publication in a future issue of this journal, but has not been fully edited. Content may change prior to final publication. Citation information: DOI 10.1109/JRFID.2017.2765619, IEEE Journal of Radio Frequency Identification

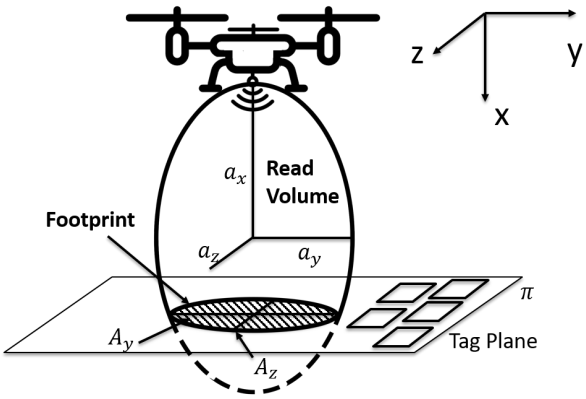

Figure 2. Ellipsoidal representation of the read volume of an RFIDrone, evaluated in the free space hypothesis, and of the footprint (axes A_y and A_z) with respect to a plane π passing through the sensors.

power sensitivities of the reader's receiver and of the tag's microchip transponder, the maximum read volume of an RFID link is related to the input power P_{in} entering into the antenna and to the above sensitivities.

Let's assume that (Fig. 2) the reader be placed at position $x = 0$ and radiating toward $x > 0$ in absence of the opposite surface, the read volume can be approximated by an ellipsoid [20] of equation:

$$\frac{(x - a_x)^2}{a_x^2} + \frac{y^2}{a_y^2} + \frac{z^2}{a_z^2} = 1. \tag{3}$$

The maximum range of the reader coincides with twice the major half-axis a_x that, for the case of forward-link is

$$a_x^F = \frac{\lambda}{4\pi}\sqrt{\chi \frac{P_{in}}{P_C} G_T G_R \tau} \tag{4}$$

and for the backward link is

$$a_x^B = \frac{\lambda}{4\pi}\sqrt[4]{\chi^2 \frac{P_{in}}{P_R} G_R^2 G_T^2 \rho} \tag{5}$$

where G_R and G_T are the gain of the reader's antenna and of the tag, τ is the power transfer coefficient of the tag, χ is the polarization loss factor of the reader-tag link (hereafter assumed equal to 0.5 without any loss of generality), ρ is the modulation depth of the chip and λ the wavelength. Depending on the specific combination of the system parameters (Fig. 3), the value of the major axis of the ellipsoid, determining the maximum link length, will be

$$a_x = min\{a_x^F, a_x^B\}. \tag{6}$$

In particular, the communication will result forward-link limited when $a_x^F \leq a_x^B$ i.e., from (4) and (5), when the following condition holds:

$$P_R \leq \frac{\rho}{\tau^2}\frac{P_C^2}{P_{in}} \tag{7}$$

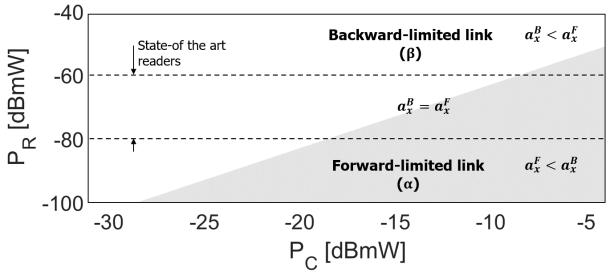

Figure 3. Graphical representation of (7) for identification of the link bottleneck. Without loss of generality it was assumed $P_{in} = 1W$, $G_R = 3dBi$, $\tau = 1$ and $\rho = 0.05$ [23].

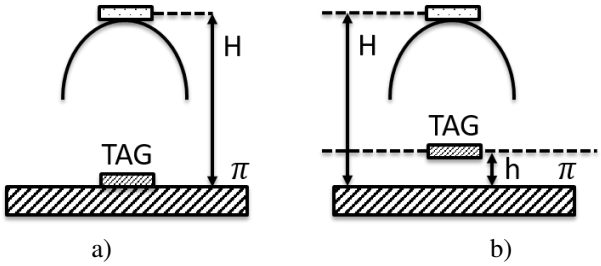

Figure 4. Definition of distances for a) tags on a surface and b) spaced-out tags.

while the bottleneck will be the backward link, within the opposite inequality. Battery-assisted tags, having high sensitivity, will generally induce a backward-limited link. New generations of passive tags fall however in the surrounding of the above condition.

The minor axes (a_y, a_z) are dependent on the major half-axis and on the radiation pattern (Fig. 4a):

$$a_\xi = a_x \sqrt{tan\frac{BW_{x\xi}}{2}\frac{sin\frac{BW_{x\xi}}{2}}{\sqrt{2} - cos\frac{BW_{x\xi}}{2}}} \tag{8}$$

where $BW_{x\xi}$ ($\xi = \{y, z\}$) are the beamwidth of the reader antenna on the principal cuts. The presence of the medium in the close surrounding of the sensor tags or hosting them can be accounted for by means of a correction to the above formula as it is shown in the following.

A. Tags-on-surface

When tags are directly attached on a locally flat surface (like a wall or the ground itself), the free-space representation of the read region in (4), (5) and (8) can be still locally applied under the condition that the realized gain of the tag $\widetilde{G}_T = G_T\tau$ in (4) is referred to the tag attached on the surface itself. The footprint is hence given by the intersection of the ellipsoid in (3) and the plane $x = H$ (Fig. 4a). Accordingly, the minor axes of the intersection ellipse are:

$$A_{y,z}(H) = \frac{a_{y,z}}{a_x}\sqrt{4Ha_x - 2H^2}. \tag{9}$$

By assuming, for the notation simplicity, that the main lobe of the reader has as circular cross-section $BW_{xy} = BW_{xz}$ and

This article has been accepted for publication in a future issue of this journal, but has not been fully edited. Content may change prior to final publication. Citation information: DOI 10.1109/JRFID.2017.2765619, IEEE Journal of Radio Frequency Identification

hence $a_y = a_z = a$, the maximum footprint size corresponds to

$$A_{max} = 2a \tag{10}$$

and is achieved when the UAV flies at the optimal distance from the surface

$$H_{opt} = a_x. \tag{11}$$

B. Spaced-out tags

In case the tags are spaced-out of a distance h from a surface (Fig. 4b) having the Fresnel reflection coefficient of amplitude Γ, the arising multi path is included in the ellipsoid model by means of a two-rays correction [20] accounting for that distance and for the reflection coefficient of the surface. By considering the only case of forward-limited links, the new major half-axis $\tilde{a}_x$ is a solution of the polynomial equation:

$$\tilde{a}_x^2 - [H + (1+\Gamma)a_x]\,\tilde{a}_x + H \cdot a_x = 0 \tag{12}$$

which yields:

$$\tilde{a}_x\,(H, \Gamma) = \frac{1}{2}\left[H + \gamma - \sqrt{(H+\gamma)^2 - 4Ha_x}\right] \tag{13}$$

where $\gamma = (1+\Gamma)a_x$. In this case, the largest footprint size can be written as

$$A_{max}(H_{opt}) = 2\tilde{a}(H_{opt}) \tag{14}$$

where $\tilde{a}$ is the horizontal axis of the corrected ellipsoid derived from (8) by replacing a_x with $\tilde{a}_x\,(H_{opt}, \Gamma)$. The optimal flight altitude H_{opt} of the RFIDrone is thus calculated by imposing that the vertical half-axis $\tilde{a}_x$ of the ellipsoid corresponds to the drone-tag distance:

$$\tilde{a}_x(H) = H - h. \tag{15}$$

By introducing (15) in (12) and solving for H, the optimal drone-surface distance is

$$H_{opt} = (\Gamma + 2)a_x + \sqrt{[(\Gamma+2)a_x]^2 + h}. \tag{16}$$

C. Parametric Analysis

The performance metrics derived above are now discussed by the help of two non-dimensional coefficients, α and β, including all power-related parameters of both the reader and the tag. The parameter

$$\alpha = \frac{P_{in}}{P_C}\widetilde{G}_T G_R \tag{17}$$

is used to characterize forward-limited links, when condition (7) is met, and the parameter

$$\beta = \frac{P_{in}}{P_R} G_R^2 G_T^2 \tag{18}$$

for backward-limited links in opposite condition.

To give a numerical meaning to the above parameters, some realistic values, corresponding to the extreme cases of battery-less sensors plus a miniaturized reader and battery-assisted sensors with a high sensitivity reader, are reported in Tab. I. Ranges $30dB < \alpha < 50dB$ and $85dB < \beta < 115dB$ look appropriate to include the state of the art of available UHF-RFID hardware.

Table I
EXAMPLES OF FORWARD- AND BACKWARD-LIMITED LINKS.

CONFIGURATION	PARAMETERS
$\alpha = 30dB$ (Battery-less Sensors, Miniaturized Reader)	Forward-limited link $P_{in} = 27dBmW$ $G_T = -1dBi$ $P_C = -4dBmW$ $G_R = 0dBi$ $P_R = -60dBmW$
$\alpha = 50dB$ (High-power reader, medium-sensitivity passive ID-only tags)	Forward-limited link $P_{in} = 30dBmW$ $G_T = -1dBi$ $P_C = -15dBmW$ $G_R = 5dBi$ $P_R = -75dBmW$
$\beta = 85dB$ (Low-sensitivity Reader and passive tags)	Backward-limited link $P_{in} = 27dBmW$ $G_T = -1dBi$ $P_C = -10dBmW$ $G_R = 0dBi$ $P_R = -60dBmW$
$\beta = 113dB$ (Reader with a high sensitivity and battery-assisted tags)	Backward-limited link $P_{in} = 30dBmW$ $G_T = -1dBi$ $P_C = -30dBmW$ $G_R = 5dBi$ $P_R = -75dBmW$

In case of battery-less tags (forward-limited links), the optimal altitude H_{opt} of the RFIDrone is only dependent on the power parameters (from (4)). For a fixed α, the footprint size increases along with the reader beamwidth (Fig. 5a). Accordingly, omnidirectional antennas are preferred over a directive one. For instance, by considering a reader's beamwidth $BW = 120°$, the arrangement of average-quality readers and tags ($\alpha = 40dB$, $\beta = 100dB$) could enable maximum footprint sizes like $A_{max} = \{2.5m, 4m\}$ in case of optimal altitude $H_{opt} = \{1m, 1.5m\}$ for forward- and backward-limited links, respectively. The upper-bound performance with state-of-the-art top-level equipments ($\alpha = 50dB$, $\beta = 115dB$) would instead permit to achieve distances up to $A_{max} = \{8m, 12.5m\}$ and $H_{opt} = \{3.2m, 5m\}$.

If tags are spaced-out from the surface, the multi path arising from the electromagnetic interaction of the reader's field with the sensors is a not-negligible cause of footprint narrowing and reduction of the optimal RFIDrone altitude (Fig. 6) that is mostly imposed by the sensor-ground distance. In the same top-class configuration as above, the expected upper-bound footprint and altitude would be $A_{max} = 2.5m$ and $H_{opt} = 1.7m$, at most.

IV. STATIC EXPERIMENTS

Theoretical achievements is here corroborated by a first preparatory experiment involving a standalone reader, i.e. in

This article has been accepted for publication in a future issue of this journal, but has not been fully edited. Content may change prior to final publication. Citation information: DOI 10.1109/JRFID.2017.2765619, IEEE Journal of Radio Frequency Identification

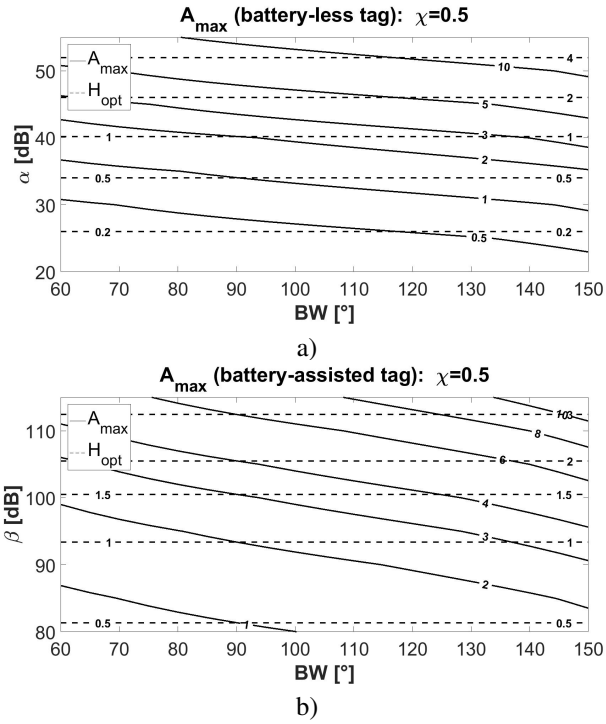

Figure 5. Tags-on-surface. Contour graphs of the optimal RFIDrone-surface distance H_{opt} and of the corresponding optimal size A_{max} of the footprint, vs. the reader antenna's beamwidth. *a*) Forward-limited links; b) backward-limited links.

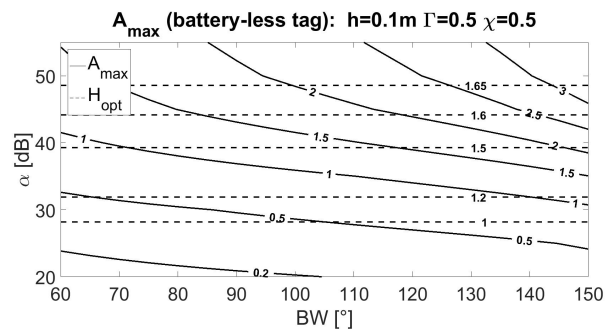

Figure 6. Spaced-out tags. Contour graphs of the optimal RFIDrone-surface distance H_{opt} and of the corresponding optimal size A_{max} of the footprint, vs. the reader antenna's beamwidth in case of forward-limited links. Tag-ground displacement $h = 0.1m$, Fresnel coefficient amplitude of the surface $\Gamma = 0.5$.

absence of a UAV, at the purpose of a precise control of the reader-surface distance. The reader was oriented in front of meadows where tags were placed spaced apart from it. Such tags were used as samplers of the reader footprint on the plane passing through them.

The reader was a CAEN Quark-UP R1270 equipped with a folded patch antenna ($G_{R,max} = 3dBi$, $BW_{xz} = 100°$ and $BW_{xy} = 130°$) fed by $P_{in} = 24dBmW$. The reader was controlled by the RADIO6ENSE Radioscan software running on a local notebook that was linked to the reader via a USB cable. Tags were Avery Dennison AD-843 dipoles with chip sensitivity $Pc = -18dBmW$ and free-space realized gain

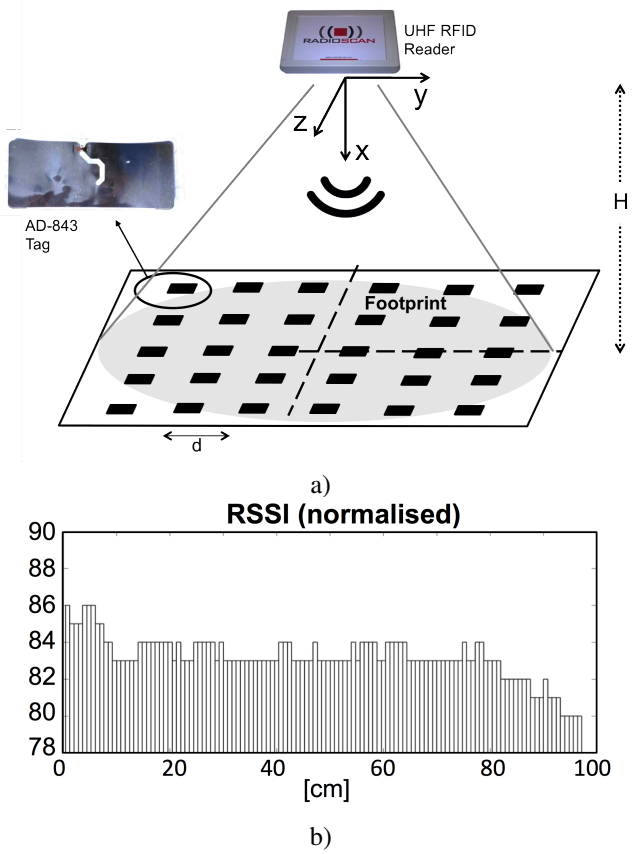

Figure 7. a) Sketch of the set-up of the static outdoor experiment over the meadows with a fixed reader and a grid of sampling tags that were 10cm spaced-out from the soil. b) An example of measured $RSSI$ of the grid tags along the y axis, in case of reader-ground level of $1m$.

$\widetilde{G}_T = -1.3dBi$. They were fixed on a plastic cloth, forming a 3 by 4 grid with inter-element spacing $d = 0.5m$. The grid was held at a distance $h = 10cm$ from the soil. The evaluation of (7) returns a forward-limited link and the non-dimensional parameter $\alpha = 44dB$ is considered. Accordingly, having assumed $\Gamma = 0.5$ for the soil [24], the optimal altitude of the reader (see the diagram in Fig. 6 for spaced-out tags) should be $H_{opt} = 1.6m$ and the corresponding maximum size of the footprint is expected to be $A_{max} = 2.2m$, i.e. close to the upper-bound values for that arrangement.

During the experiment, the reader was held on a dielectric mast and moved along the two symmetry axes of the array at heights $H = \{0.5,\ 1,\ 1.5,\ 2\}m$ from the ground. Accordingly, maps of the Received Signal Strength Indicator (RSSI) were recorded as in Fig. 7b. The footprint's boundary is hence identified as the cut-off of the RSSI trace. The experimentally estimated maximum footprint diameter was $A_{max} = 2m$ corresponding to a optimal height $H_{opt} = 1m$: these results are coherent with the above theoretical results.

V. Flying RFIDrone

More realistic experiments concerned the use of a FlyTop FlyNovex drone having 7 kg net weight, 4 kg maximum payload, 20 minutes of autonomy and capable to fly at up to

This article has been accepted for publication in a future issue of this journal, but has not been fully edited. Content may change prior to final publication. Citation information: DOI 10.1109/JRFID.2017.2765619, IEEE Journal of Radio Frequency Identification

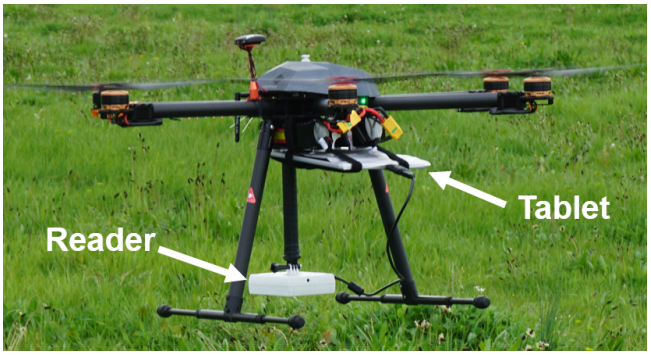

Figure 8. Drone FlyTop FlyNovex hosting a tablet and a compact Reader connected to a polyethylene mast.

50 km/h (Fig. 8). The same compact reader as above was this time paired, and also powered, with an Acer Aspire Switch Laptop forming an all-in-one interrogating unit with overall weight of about 1.5 kg, suitable to be installed onboard the UAV without tethering to a ground station. In particular, the reader was hung to a polyethylene hollow tube while the tablet was fixed just below the UAV. Both battery-less and battery-assisted tags were used in two different experiments.

A. Numerical model of the RFIDrone system

The reader-drone system was preliminary modeled by means of the Method of Moments (FEKO implementation) at the purpose to derive the embedded maximum gain and beamwidth of the reader to be inserted in the parametric model in Section III. A simplified, but representative version of the UAV airframe (Fig. 9a) includes a Carbon Fibre structure (conductivity $\sigma = 4000\,S/m$ [25]), while extra conductive parts (i.e. the batteries and the tablet) are accounted for as perfect conductors. A detailed model of the reader's folded antenna is also included in the simulation.

The numerically estimated onboard antenna pattern (Fig. 9b) is more directive ($G_{R,max} = 6dBi$, $BW_{xz} = 79°$ and $BW_{xy} = 71°$) and with a better front-to-back ratio w.r.t. the standalone patch antenna in the previous experiment as a consequence of the electromagnetic interaction with the carbon fiber body of the UAV. In particular, intermediate simulations of the RFIDrone revealed that the legs of the structure produces a narrowing of the beam (especially on the zx plane).

Finally, for the considered system parameters ($\alpha = 47dB$, $h = 10cm$ and $\Gamma = 0.5$), the theoretical model in Section III (Fig. 5b) returned an optimal drone-level distance $H_{opt} = 1.6m$ and the largest footprint size $A_{max} = 1.5m$. As expected by the more directive reader antenna pattern, A_{max} is a few smaller than in the case of standalone reader in Section IV.

B. Experiments with a grid of Battery-less spaced-out tags

A grid of 4 by 7 AD-843 tags (inter-element spacing $d = 0.5m$) was placed again at a distance h=10cm from the meadow (soil level) as in Fig. 10a. Accordingly, the drone was driven in order to fly over the grid along the y direction to scan

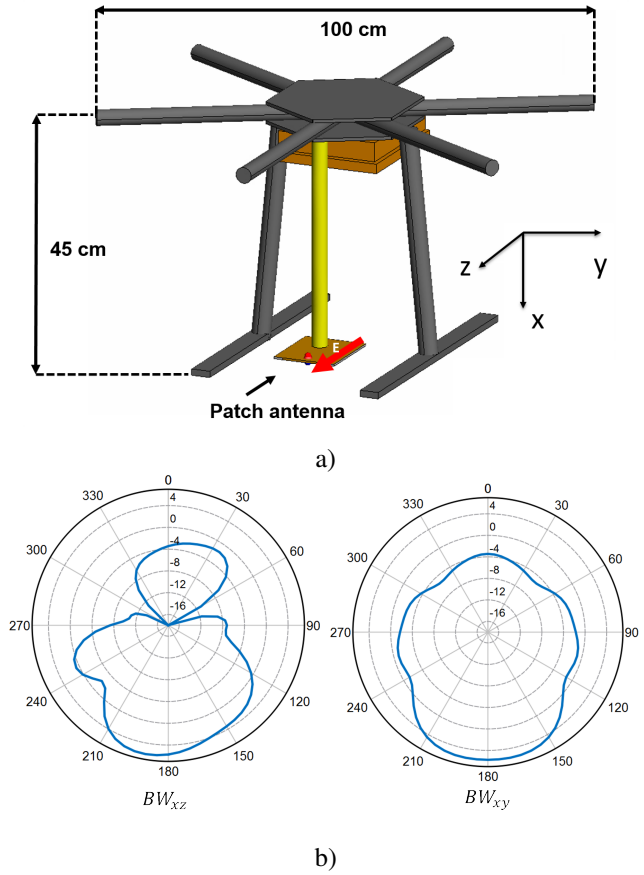

Figure 9. a) Simplified electromagnetic model of the RFIDrone. b) Gain (at $870MHz$) on the E-plane (BW_{xz}) and H-plane (BW_{xy}) of the radiation pattern of the onboard folded patch antenna of the reader

the tags from different altitudes $H = \{0.5,\ 1,\ 1.5,\ 2\}m$ and speed $v = 0.5m/s$. During the flight, the drone collected the RSSI of the instantaneously responding tags. As an example, Fig. 10b shows the snapshots of the RSSI that was measured when the drone approached the up-left corner of the array. The altitude corresponding to the maximum average number $N_{FP} = 5$ of instantaneously read tags was $H_{opt} = 1m$ and accordingly, the maximum footprint was $A_{max} = 1m$. The experimental footprint and distances are still close to the expected theoretical values in spite of the uncertainty in the control of the UAV trajectory and of the coarse discretization of the sampling surface.

It is worth reporting that, by moving the tags directly down to the meadows, a huge degradation of their realized gain was produced and hence it was not possible to test the on-surface configuration. Anyway, in case the same gain of the spaced-out alignment was preserved, the on-surface deployment could be interrogated, according to the theoretical model, within a much larger footprint $A_{max} = 5m$ (for $H_{opt} = 1.8m$).

Finally, the reading reliability was evaluated by repeating the scan from the optimal height $H = 1m$ and for different velocity of the UAV $v = \{0.5,\ 1,5,\ 2\}m/s$. The number of read tags were instantaneously recorded and the hit rate

This article has been accepted for publication in a future issue of this journal, but has not been fully edited. Content may change prior to final publication. Citation information: DOI 10.1109/JRFID.2017.2765619, IEEE Journal of Radio Frequency Identification

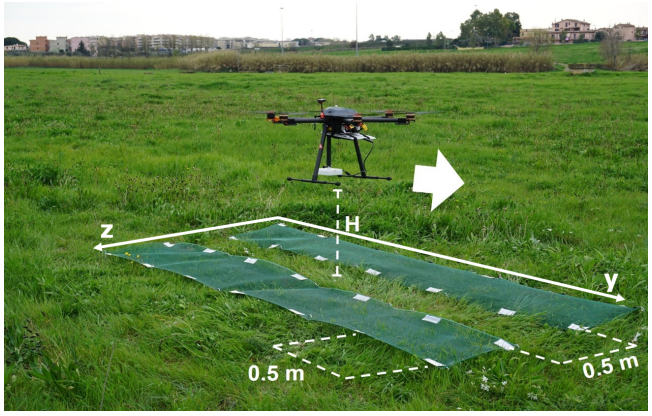

a)

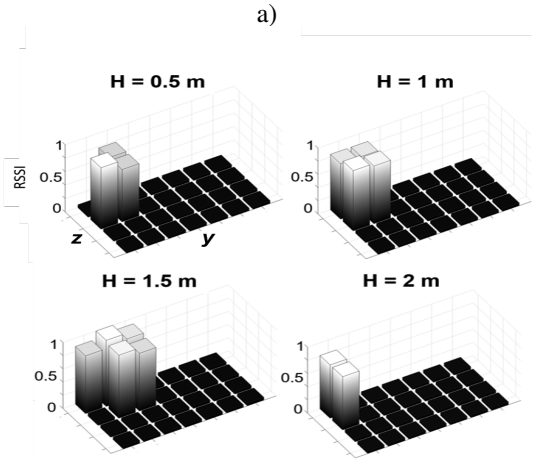

b)

Figure 10. a) Flighting RFIDrone experiment with a 4 by 7 array of battery-less AD-843 tags over meadow; b) examples of snapshots of the instantaneously measured (normalized) $RSSI$ data that collected by the RFIDrone while approaching the top-left of the grid at different heights.

$HR(v)$ was hence computed as in (1) with $N_{FP} = 5$. Results in Tab. II say that the reading reliability reduces with increasing flight speed so that the system becomes un-reliable for a velocity $v > 1.5m/s$.

Table II
HIT-RATE IN THE SCANNING OF THE TAG MATRIX FROM ALTITUDE $H = 1m$.

Speed	HR(v) [%]
Low (0.5 m/s)	90
Medium (1.5 m/s)	60
High (2 m/s)	18

C. Experiment with a BAP on-surface tag

In the last test, a battery-assisted tag based on the RADIO6ENSE T-card temperature sensor (Fig. 11) is considered. The tag is made of a planar slot connected to the EMemectronics EM4325 RFID microchip that is capable to switch to a high sensitive threshold power ($P_c = -31dBmW$) if used in BAP mode. The presence of a metallic back-shielding makes this tag suitable to direct application over any medium.

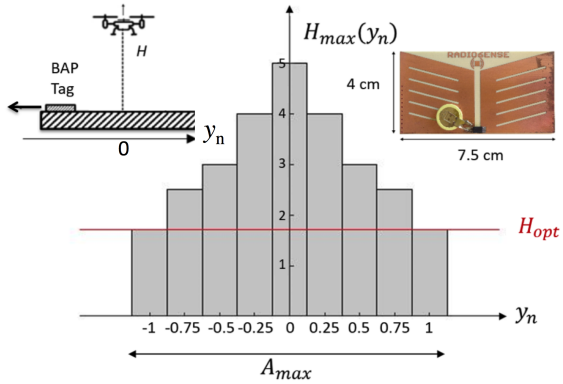

Figure 11. RFIDrone with BAP-tags ($P_C = -30dBmW$, $\widetilde{G}_T - 2.5dBi$) directly placed on a paved clearing. Bars represents the measured maximum height of the UAV for increasing distances of the BAP-tag from the UAV projection. Left inset: the mutual drone-tag position. Right inset: the BAP tag.

The reader was the Thing Magic M5e having sensitivity $P_R = -70dBmW$, connected to the same folded patch as above ($G_{R,max} = 6dBi$) fed by $P_{in} = 27.5dBmW$.

This time, the experiments were performed with the tag placed on the ground and the measured embedded realized gain was $\widetilde{G}_T = -2.5dBi$. In this condition, this link is backward-limited with a corresponding power parameter $\beta = 104dB$. The expected maximum footprint size and the optimal height are$A_{max} = 2.8m$ and $H_{opt} = 1.7m$, respectively.

As only a single BAP tag was available, the experimental estimation of the corresponding parameters was carried out according to the following procedure. The tag was moved along a line centered at the drone projection on the ground. For each position y_n of the tag the drone was raised up vertically until the tag stopped responding so that a $H_{max}(y_n)$ bar diagram is obtained. Fig. 11 permits to identify the maximum footprint as $A_{max} = 2.2m$ and the optimum height $H_{opt} = 1.7m$ still in reasonable agreement with the theoretical values.

VI. CONCLUSIONS

The capability of a flying drone equipped with an RFID reader to scan sensor tags displaced onto or close to surfaces has been quantified by means of the read footprint indicator. Theoretical as well as experimental investigations demonstrated that there exists an optimal flying distance of the drone from the surface such to maximize the footprint size which could be 9-12m large in case of state-of-the-art readers and battery-less or battery-assisted tags. The optimal altitude is of the order of 3-5m for forward- or backward-limited RFID links, respectively. Worse footprints are instead estimated when sensor tags are spaced apart from the surface (roughly one third of the above sizes for *h*=10cm) due to the destructive effect of the multi-path.

In general, as the maximum permitted radiated power is limited by local regulations, the maximum reading distance

can be improved by using tag antennas with higher directivity without impacting on the local regulations or by using reader antennas with higher directivity and by decreasing the reader's emitted power. Instead, the increase of the maximum footprint, as requested to speed-up the scanning of surfaces, can be only achieved by the combined improvement of both the sensitivity of reader's receiver and of tag's microchips.

The communication performance is moreover sensibly affected by the flying velocity of the drone so that the Hit-rate degrades down to 50% for velocity more than 1.5m/s.

The presented analysis was restricted to RFIDrones scanning a ground surface while other interesting configurations involve tags displaced over a vertical surface so that the onboard antenna has to be differently arranged. Further investigation is hence required to define proper arrangement of the reader's antenna also accounting for the close interaction with the drone airframe which has a not negligible impact on the size of the read footprint.

Acknowledgment

Authors wish to thank the two University spin-off GEO-K (www.geo-k.co) and RADIO6ENSE (www.radio6ense.com) for hardware and software support.

References

[1] S. Amendola, M. C. Caccami, A. Caponi, L. Catarinucci, V. Cardellini, E. Di Giampaolo, S. Manzari, F. Martinelli, S. Milici, C. Occhiuzzi, and G. Marrocco, "RFID & IoT: a Synergic Pair", *IEEE RFID Virtual Journal*, N.8, Mar 2015S.

[2] Gupte, P.I.T. Mohandas and J.M. Conrad, "A survey of quadrotor Unmanned Aerial Vehicles", *Proceedings of IEEE*, pp. 1-6, Mar. 2012

[3] J. Wang, E. Schluntz,B. Otis, T. Deyle, "A New Vision for Smart Objects and the Internet of Things: Mobile Robots and Long-Range UHF RFID Sensor Tags,", *arXiv preprint whitepaper,* no. 1507.02373, Jul. 2015, available at: http://arxiv.org/pdf/1507.02373.pdf

[4] G. Greco, C. Lucianaz, S. Bertoldo, and M. Allegretti, "A solution for monitoring operations in harsh environment: a RFID reader for small UAV", in *Electromagnetics in Advanced Applications (ICEAA), 2015 International Conference on*, pp. 859-862, Sept. 2015

[5] M. Allegretti, S. Bertoldo, "Recharging RFID Tags for Environmental Monitoring Using UAVs: A Feasibility Analysis," *Wireless Sensor Network*, pp. 13-19, Feb. 2015

[6] "Futuristic Inspections for Bridge Safety", *TuftsNow*, Tufts University, May 2014, available at: now.tufts.edu/articles/futuristic-inspections-bridge-safety

[7] "Drone Tech and Atkins develop UAV RFID system", *ADS Advance*, April 2016, available at: adsadvance.co.uk/drone-tech-and-atkins-develop-uav-rfid-system.html

[8] G. Greco, C. Lucianaz, S. Bertoldo, and M. Allegretti, "Localization of RFID tags for environmental monitoring using UAV", in *Research and Technologies for Society and Industry Leveraging a better tomorrow (RTSI)*, *IEEE 1st International Forum on*, pp. 480-483, 2015

[9] "The flying inventory assistant", Fraunhofer Institute for Material Flow and Logistics IML, Dec. 2014, available at: www.fraunhofer.de/en/press/research-news/2014/december/the-flying-inventory-assistant.html

[10] B. Hubbard, H. Wang, M. Leasure, T. Ropp, T. Lofton, S. Hubbard, and S. Lin "Feasibility Study of UAV use for RFID Material Tracking on Construction Sites", in *51st Associated Schools of Construction Annual International Conference Proceedings,* 2015

[11] D. Mascareñas, E. Flynn, M. Todd, G. Park, C. Farrar, "Wireless sensor technologies for monitoring civil structures", *Sound and Vibration,* no. 42, pp. 16-21, Apr. 2008

[12] DroneScan - Airborne Inventory and data collection, available at www.dronescan.com

[13] UAV SmartHub™, a Complete Smart Cloud Solution for Scanning RFID, Bluetooth & Smart Sensors with any commercial grade UAV/Drone, available at www.dronesmartx.com

[14] DeltaDrone - Robotic barcode scanning for large uniform warehouses, available at www.deltadrone.com

[15] "ITL-DRONE (Identificación Trazabilidad y Localización mediante DRONES con tecnología RFID)", *Tag Ingenieros*, Oct. 2015, available at: www.tagingenieros.com/?q=node/197

[16] C. Swedberg, "RFID-Reading Drone Tracks Structural Steel Products in Storage Yard", *RFID Journal*, Sept. 2014, available at www.rfidjournal.com/articles/view?12209/

[17] "Kenyan reserve sheltering rare rhinos to launch anti-poaching drone", *Wired Technology*, Jul. 2013, available at www.wired.co.uk/news/archive/2013-07/29/anti-poaching-drone-kenya

[18] M. Longhi, G. Casati, D. Latini, F. Carbone, F. Del Frate and G. Marrocco, "RFIDrone: Preliminary Experiments and Electromagnetic Models", *URSI Int. Symp. on Electromagn. Theory (EMTS)*, Aug. 2016

[19] T. Deyle, M. S. Reynolds, and C. C. Kemp. "Finding and Navigating to Household Objects with UHF RFID Tags by Optimizing RF Signal Strength.", I*EEE/RSJ International Conference on Intelligent Robots and Systems*, 2014

[20] G. Marrocco, E. Di Giampaolo, R. Aliberti, "Estimation of UHF RFID Reading Regions in Real Environments", *IEEE Antennas and Propagation Magaz.*, Vol. 51, pp. 44-57, Dec. 2009

[21] J. A. Singh, C. Deupser, E. Olsen and S. P. Singh. "An Examination of the Variables Affecting RFID Tag Readability in a Conveyer Belt Environment", *Journal of Applied Packaging Research,* Vol. 2, N. 2 p. 61 - 73, 2007

[22] L. W. Mayer, *Antenna design for future multi-standard and multi-frequency RFID systems*, Thesis dissertation at Technical University of Wien, Jun. 2009, available at publik.tuwien.ac.at/files/PubDat_176539.pdf

[23] L. W. Mayer, A. L. Scholtz, "Sensitivity and Impedance Measurements on UHF RFID Transponder Chips", *Proceedings of the second international EURASIP workshop on RFID technology*, Budapest. 2008.

[24] F. T. Dagefu, K. Sarabandi, "Soil dielectric and sensitivity analysis for subsurface imaging applications based on distributed Sensor Networks", *IEEE International Geoscience and Remote Sensing Symposium (IGARSS)*, Jul. 2010

[25] "The Effect of Carbon Fibre Body Panels on Aircraft RCS", *FEKO Whitepaper*, available at www.feko.info/applications/white-papers/the-effect-of-carbon-fibre-body-panel-on-aircraft-rcs/the-effect-of-carbon-fibre-body-panel-on-aircraft-rcs